OPAL-A - THE FIRST 100 DAYS

B.Y. SMITH', K.A. RODGERS[1,2] & P.R.L. BROWNE[1, 3]

'De artment of Geology, University of Auclcland, Private Bag 92019, Auckland
'Research Associate, Australian Museum, Sydney, NSW 2000, Australia
[3]Geothermal Institute, University of Auckland, Private Bag 92019, Auckland

SUMMARY – Samples of silica sinter, <2 years old taken from the discharge drain of the Wairakei Power Station and the sinters terraces of Orakei Korako, all consist of non-crystalline opal-A. Initially silica deposited in the Wairakei drains forms a mat woven from strands (36μm long, 0.4 mm diameter) of smooth non-porous opal-A in which most strands are aligned parallel to the current but some protrude above the mat surface. The silica of the strands rapidly forms chains of oblate, coalesced microspheres <0.4x0.2 μm. Following deposition the width of the opal-A x-ray scattering broadband at quarter (FWQM) half (FWHM) and three quarter (FWTM) of the maximum intensity decreases slightly. Samples younger than 0.1 years display the highest FWQM, FWHM and FWTM values. Opal-A silica continues to precipitate and mature following removal from the parent fluid, so long as the sinter surface is filmed by water. A continual movement of silica is shown by a second generation of microspheres formed on the mat surface, by an increase in size of the initial microspheres, and by an increase in maximum intensity of the x-ray scattering bands. These changes accord with the known behaviour of juvenile opaline silica in both natural and artificial systems whose pH, temperature and dissolved salt content are similar to Wairakei and Orakei Korako e.g. gelling of silica is favoured by the high pH and temperature of the Wairakei discharge fluid with the high dissolved salt content of the water essential for solid silica to accumulate within the drain.

1. INTRODUCTION

When first deposited, sinter from near-neutral alkali chloride waters consists of opal-A, a non-crystalline, hydrated silica phase. Herdianita e? al. (2000a) found that with time, opal-A transforms into paracrystalline opal-CT and/or opal-C, and, subsequently, recrystallises to quartz. The maturation process typically takes 50,000 years and is expressed in changes in the physical properties and textures of the silica phases.

In Herdianita's et al. (2000a) model of sinter aging, all samples of opal-A younger than lyear were plotted on a single, year-1 time line i.e. no indication was given as to whether any of the physical parameters affecting the opal-A changed during the first year. However, they recorded a wide spread of values in the properties of these young samples so the present study was undertaken to evaluate whether these ranges might reflect processes occurring soon after initial deposition.

2. SAMPLE OCCURRENCE

Samples are categorised into 3 groups (Table 1).
Group A An unlimited supply of fresh opal-A is available from the concrete drains used to discharge waste water from the bore field. Thick deposits, typical of streamer microfacies silica, accumulate at a rate of several cm per year in these drains that consist of two adjoining concrete channels each 1.5m wide. A central divider that separates the channels was originally intended to permit each to be used independently but ground subsidence has caused the hot water to overtop this divider. Flow rate is now about 550 l/s with water cooling from 95°C at input to about 70°C at the drop structure.

A large sample was taken of the fresh, well-developed streamer microfacies growing on the central divider (sample # WKdrfresh; Fig. 1). Immediately following collection, it was placed in a clean container filled with discharge water, that, at the time of sample collection, had a temperature of 62.5 °C and a pH of 8.3. Subsequently, portions of this sample were removed from the water and air dried at room temperature for differing periods. These intervals are denoted by the numerical suffix attached to the sample number e.g. 6h = 6 hours, 3d = 3 days. A minimum of six hours was needed to air dry the sample sufficiently for physical analysis and this sample has been taken as the benchmark of fresh, unaltered silica sinter for the purposes of this study.

Group *B* The build up of silica is such that the drains become clogged and require cleaning so silica towards the end of the streamers is presumably very young. In addition, sinter samples were available from the last clearing of the drain about 3 months previously (R. Smith, pers comm.). These had been left on the bank beside the drain and, as such, represent slightly weathered,

albeit very young, silica streamer microfacies. All appeared to consist of massive sinter scraped from the walls of the discharge sluice. These have been therefore assigned an age of ≤0.3 yr.

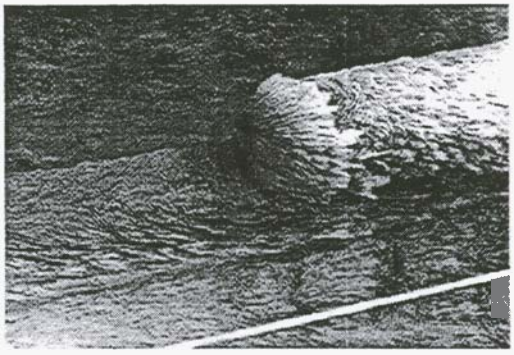

Fig. 1. Streamer fabric silica actively depositing in the Wairakei discharge drain. Flow is from left to right.

Group C In addition to this artificial depositional environment, comparative examples of young, naturally-occurring silica sinter were taken from the large sinter terraces of Orakei Korako. One sample, S21(3), was taken fiom the uppermost surface of a fresh bubblemat currently undergoing silicification. It is very young, comparable to very fresh Wairakei drain sinter, –0.1 yrs.

In the absence of appropriately aged older sinter of the streamer facies, examples were taken of both palisade and bubblemat microfacies and include DT1a & b from the top 10 mm of sinter, Oktutu6 fiom a recent, totally silicified surface bubblemat containing numerous large voids, and S21(2)a and S22(2) from totally silicified top laminae that occurs on bubblemats at the air/water interface with S21(2)b taken from layers of smooth non-porous silica immediately below S21(2)a. Given the position these samples occupy within the sinter aprons and the known rates of sinter accumulation at Orakei Korako (Lloyd, 1972), all are regarded as being >1 yr but ≤2 yr old. These samples represent the second end member in the present study - complementing WKfresh and S21(3). Importantly, none had suffered any alteration from post-depositional steam heating.

3. METHODS

Of the different physical properties of silica sinter phases found to vary with age by Herdianita *et al.* (2000a) the most sensitive response was in the size and shape of the x-ray scattering broadband used to compare the degree of lattice disorder of individual opal-A specimens. The most convenient property of this band used by Herdianita *et al.* (2000a,b) was the full width at half maximum (FWHM), an approach analogous to that used to evaluate the crystallinity of some clays. It has been adopted here to appraise the different opal-A at various stages of the aging process and to enable direct comparisons to be made with the Herdianita *et al.* (2000a) maturation model. However, in the present study it was also found useful to compare the full width at quarter maximum (FWQM) and full width at three quarter maximum (FWTM), along with the position and intensity of the scattering maximum, to better compare the size and shape of the different bands. All samples were scanned by a Philips X-ray Diffractometer using the same instrumental settings and experimental constraints as determined by Herdianita *et al.* (2000b).

Along with the variation in physical properties, progressive changes occur in the morphology of the different textural components of the sinter at an ultrastructural level. Each of the samples was examined by a high resolution scanning electron microscope (SEM) to see if any consistent changes were apparent in the first year of opal-A's existence.

4. RESULTS

Mineralogy

All samples showed the characteristic x-ray scattering broadband of opal-A (*cf.* Smith, 1998; Herdianita et *al.*, 2000a,b) - the dominant phase present. The scattering bands of all samples in the 3 groups are highly symmetrical, as is typical among opal-A that has not been subject to post-depositional heating or advanced weathering. The FWQM, FWHM, and FWTM of the youngest sample (WKfresh6h) show values higher than most other samples in Group A (Table 1), implying that changes occur in the opaline silica immediately it is removed from the parental water. Uncertainties in the precise age of the samples contributes towards the spread of measured values in halfwidths. However, overall the halfwidth values of the Group A and B samples, and the very young Orakei Korako silica, lie towards the upper end of the range of the youngest samples cited by Herdianita *et al.* (2000a) and are greater than Group C samples, with the exception of Dt1a, possibly the youngest sample of that Group (Fig. 2). Along with changes in the broadband shape is a sympathetic decrease in the maximum intensity of the scattering broadband over the first 40 days following removal from the parental water. Thereafter the intensity increases until it eventually exceeds that of the initial 6 hour value. The maximum intensity continues to increase with time and Group A (<0.1 yr), Group B (<0.3 yr) and Group C (>1, < 2 yr), display maxima having 92, 98, and 108 counts/sec, respectively (Fig. 3) i.e. the increase in maximum intensity increases very rapidly.

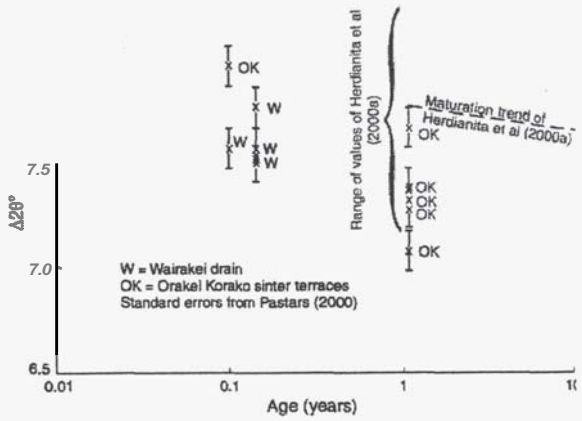

Fig. 2. Extension of the sinter aging model of Herdianita et.al. (2000a) using FWHN data from present study

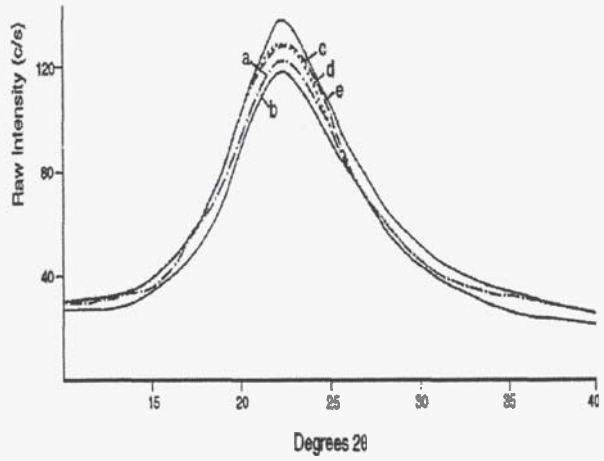

Fig. 3. Representative, highly smoothed, x-ray powder scattering bands for young sinters from the Wairakei discharge drain and from terraces at Orakei Korako: (a) fresh sinter, Wairakei discharge drain; (b) six week air dried sinter, Wairakei discharge drain; (c) 5 month air dried sinter, Wairakei discharge drain; (d) very young bubble mat facies, Rainbow terrace, Orakei Korako; (e) young bubble mat facies, Rainbow terrace, Orakei Korako.

Ultrastructure

Group *A:* At an ultrastructural scale, the first deposited silica of the Wairakei drain forms a densely-packed mat woven from smooth strands of opal-A that are generally aligned parallel with the flow direction (Fig. 4a). Some strands criss-cross forming a weft to the main strands warp. In places, occasional strands protrude above the surface of the main mat. The majority of individual strands are <8.0 μm long but some grow as large as 55 μm. Strand diameter is typically 0.4 μm but may be up to 1.0 μm where several strands from side by side. Under high magnification e.g. >50,000x, some strands are seen to consist of an agglomeration of very small nanospherical particles <300 nm in diameter.

Following formation of the initial silica, deposition continues and transforms the strands into a series of juxtaposed, coalesced, oblate, opal-A microspheres (0.2x0.4 μm). Only in a few strands is the substructure of coalesced nanospheres obvious. Further deposition give the strands a somewhat irregular, lumpy appearance (Fig. 4b). A second generation of occasional, well-formed, small (~0.4 μm diameter) opal-A microspheres are scattered across the mat surface. Voids between strands have a maximum size of 5x2 μm, and occur where strands bifurcate at an angle of 45° from the principal direction of strand alignment.

Euhedral halite crystals, <1.5 μm along the cube edge, litter the surface of the SEM mount and have presumably crystallised from residual, drain parent alkali-chloride brine upon air drying of the sample. Diffraction lines of halite occur in XRPD scans of all Group A but not in Group B samples, where any traces of the parent fluid may have been washed out by rain.

Group *B:* Five month old streamer microfacies has a similar general habit to the opal-A of fresh Group A streamer microfacies. Opal-A spheres again form chains of oblate, coalesced microspheres, but average sphere size in Group B samples is now up to 1.8 μm diameter. The sphericity of these microspheres is more pronounced than in Group A such that the Group B strands often resemble a string of beads. In places individual spheres forming the silica strands have become obscured by a silica overgrowth.

As in Group A, a second generation of well-formed opal-A spheres, up to 0.5 μm across, nestle in hollows of the primary silica mat and their occurrence is taken as indicating that opal-A continues to precipitate after the sinter is removed from the drain fluid. It is amongst Group B samples that a higher maximum intensity of the v opal-A x-ray scattering band occurs and this increase is taken as denoting an initial maturation of the juvenile silica, occurring in the first 16 weeks following deposition.

Wallrock: In sample Wkdrwall from the horizon directly adjacent to the drain wall (Zone 1) i.e. the oldest, consists of closely-packed silica strands aligned both with one another and the flow direction; the close-packing of the silica strands is what gives the sinter its coherency. An undulating and gradational contact occurs between this wall-attached layer and the next silica layer away from the wall (Wkdrwal2, Zone 2) which varies in thickness from 2-10 mm. Silica forming this second horizon consists of strands with no preferred orientation. There is no cementation of the strands but the sinter is bound together by numerous overlaps similar to those shown in Fig. 4a. Beyond Zone 2, the sinter takes on the typical streamer fabric appearance aligned with the flow direction (Zone 3) with individual strands up to 20 mm long.

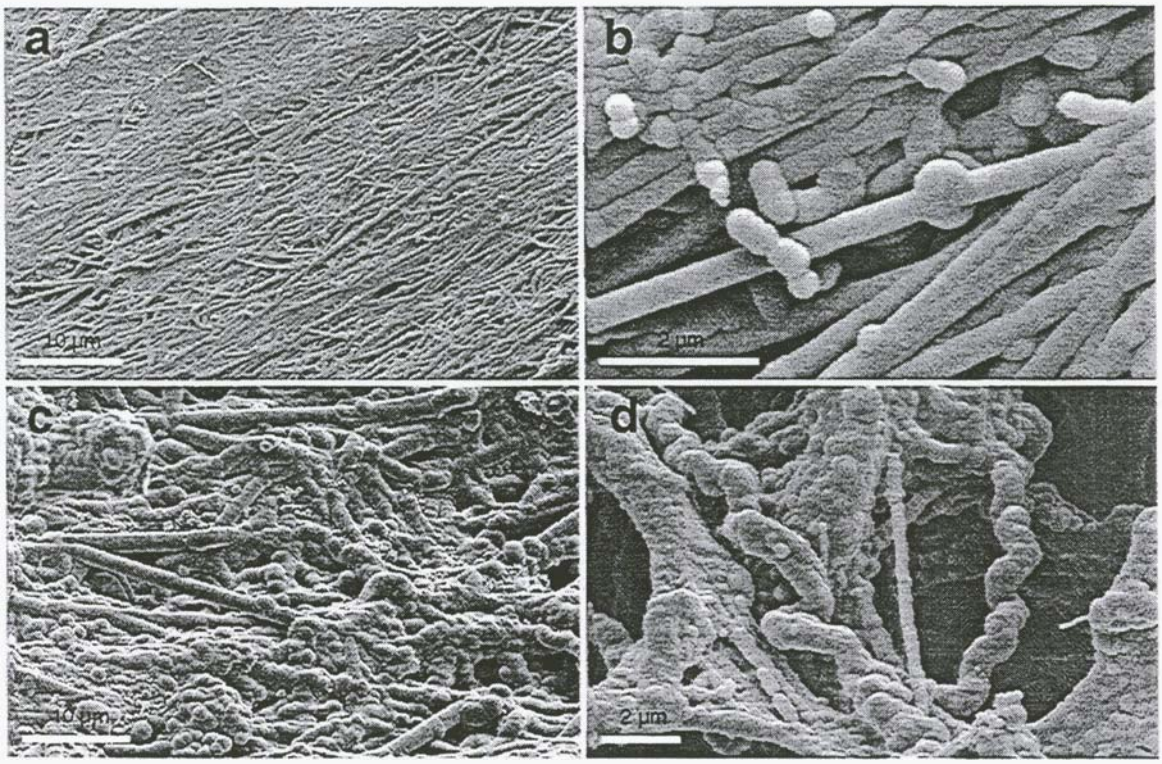

Fig. 4. Scanning electron microscope images of sinter, Wairakei discharge drain, (a, b, d) fresh sinter, air dried for 3 days; (c) ex-drain < 0.3 yr; (a, 3b) densely-packed mat of silica strands, generally aligned in flow direction, and with *cross* strands forming a weft to warp of main strands; (b, 3c) strings of oblate opal-A microspheres in wrapping around smooth non-porous strands, transforming them into lumpy smooth non-porous strands; (c, 4a) closely-packed, smooth, non-porous silica strands in which individual microspheres are becoming more spherical and increasing in size; (d, 5c) clockwise helical silica strands.

These drain samples indicate that current flow can exercise a profound effect on the habit of the silica (Fig. *5).* Initially, on the flat drain surface, silica deposits as strands aligned and oriented with the flow direction (Zone 1) but as the sinter thickness increases differential deposition of silica occurs (Zone 2) to produce the gradational and undulating contact between Zones 1 and 2. This could occur where low amplitude standing waves develop in the flow along the walls at this point, producing small variations in current velocity and direction and produce an undulating surface on the deposit at the solution/substrate interface. Deposition occurs with no preferred orientation to the strands with respect to the dominant flow direction. Where turbulence and eddies occur between undulations, clockwise helical strands form (Fig. 4d). Further out in the current, where the flow is undisturbed by drag along the wall, the strands of silica grow in the principal flow direction.

Group *C:* Opal-A spheres in the <2 year old sinter of Orakei Korako Group *C* samples possess the habits typical of silica deposited upon a microbial substrate (e.g. Rodgers, 2000). Well-formed, opal-A spheres, <1 µm diameter, coalesce about the microbial filaments (Fig. 6b). Elsewhere, individual microspheres, occur in botryoidal clusters. The proportion of well-formed opal-A spheres increases with increasing age.

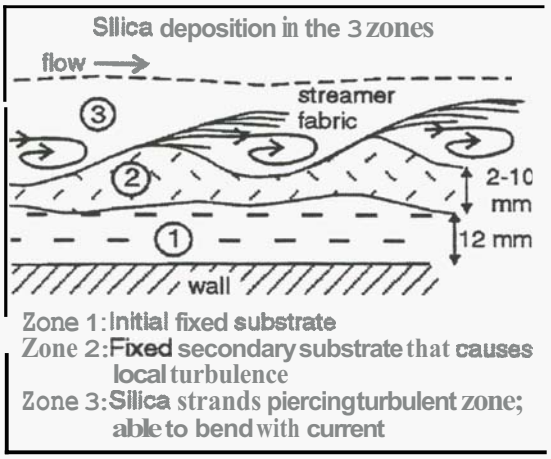

Fig. 5. Schematic interpretation of the effect of turbulence on silica deposition.

5. DISCUSSION

The development of opal-A and the ensuing changes observed in the crystal chemistry and texture following deposition and subsequent removal from its parent fluid, are consistent with what is known of the behaviour of silica in both natural and artificial systems of comparable pH,

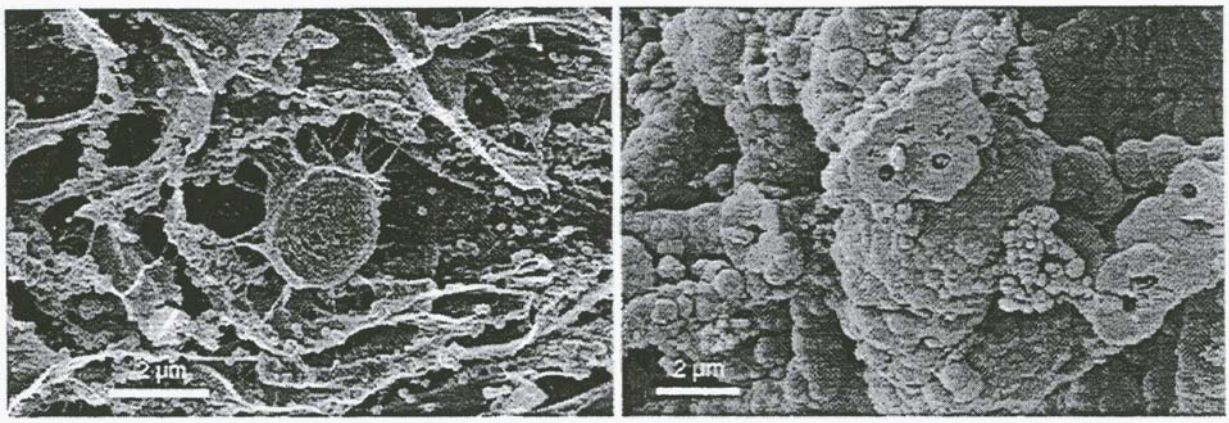

Fig. 6.(a) Dispersed opal-A spheres, < 1µm diameter, both silicifying and clustering on surface of microbial filament; (b) Scanning electron microscope images of young sinter, <2 yrs old, Orakei Korako.

temperature and dissolved salt content to the Wairakei and Orakei Korako parent fluids.

In the first instance, for silica to flocculate from the Wairakei discharge water, under the prevailing pH and temperature conditions, the presence of dissolved ions, such as Ca and Na, is essential. Above a pH of 6, pure silica sols are relatively stable. All silica particles, including oligomers, bear a negative charge and mutually repel one another. With increasing pH, there is a decrease in the number of interparticle collisions, and hence in opportunities for adhesion and growth. Coagulation, i.e. growth of such particles that may lead to flocculation, occurs readily where particle-particle interaction is afforded by residual bonds or some other form of particle-particle bridging. This can occur in the presence of coagulants such as salt cations or organic molecules. Iler (1979, p.376) states that, "in *all* cases, flocculation is due to interparticle bonding through the cations." He illustrates this with specific reference to the role that Na^+ can play (Fig. 4.17a, p.377), arguing that coagulation can occur as soon as sufficiently ion-exchanged sodium has been absorbed on to the surface of each silica particle. It is the levels of Na^+ and Ca^{2+} in the Wairakei discharge that facilitate flocculation and rapid build up of the silica in the drains despite the high pH and water temperature that favour gelling. In contrast, at Orakei Korako where the parent fluid is dilute, sinter grows more slowly, particularly away from the vent out on the sinter aprons. It is subtle variations in dissolved salt concentration, pH, temperature and the presence or absence of organic/biological molecules that will determine whether the coagulum gels or develops as a solid phase (e.g. Iler, 1979 pp. 364-407). Typically, silica colloids are <5 nm. As they aggregate the radius of curvature increases and the surface of the growing particle tends to fill where small colloid particles adhere to a surface rather than one another. It is an extension of this process that produces the microsphere structure and nanosphere substructure of the juvenile Wairakei silica strands.

All samples examined show a limited range in particle size and shape. Once silica particles grow to a certain size, there is very little change in energy content with surface area (Iler, 1979). There is thus an optimum upper limit on the size to which particles may grow, at least in the initial stages of deposition. Further, when growth continues following adhesion, larger particles grow at the expense of smaller, that are consequently eliminated. The two processes, acting in tandem, limit the range in microsphere size of the end product.

Deposition occurs preferentially upon surfaces having minimum radius such as where two particles are in contact (Iler, 1979) and it is this process that yields the continuum of textures seen in the Wairakei samples: individual particles → juvenile strands → bead strings → irregular lumps. Growth will continue so long as a film of water is present on the sinter surface e.g. pore water. Such a film allows activity gradients to become established and maintained in order to facilitate the movement of silica (Landmesser, 1995). Importantly, unlike other metal oxides, the solid silica remains non-crystalline throughout and enjoys an appreciable solubility in water, thus facilitating post-depositional growth and textural changes. The efficacy of the silica deposition process and the strength of the residual bonds that link the microspheres is reflected in the rapid build up of silica on all available surfaces throughout the Wairakei drain, despite the speed and turbulence of the discharge water.

The variations observed in the size and shape of the x-ray scattering broadband are also consistent with established models of changes in young non-crystalline silicas. When first removed from its parent fluid, opaline silica loses water and its

juvenile, open structure collapses (Iler, 1979). Presumable it is this change that is reflected in the initial reduction in FWQM, FWHM, and FWTM. Subsequently, as the scattering intensity increases and the half widths decrease further, if, as in clays, the half width is taken as a measure of lattice disorder, then a small reduction in the disorder of the opaline structure is implied during the earliest maturation of the deposit. Certainly, the half width changes observed in the present study are consistent with the pattern of behaviour found by Herdianita *et al.* (2000a) who reported a overall decrease in FWHM with time, and the results extend the range of their aging model by two orders of magnitude (Fig. 2). Regardless of post-depositional changes, both the Orakei Korako and Wairakei samples retain a high level of porosity. Deposition of the colloid is accelerated and the deposits can become dense and hard when soluble silica is deposited along with colloidal particles. As the solution cools the colloidal particles first deposit on available solid surfaces. At the same time the cooling solution becomes oversaturated with respect to soluble silica and it is this silica that subsequently deposits upon and cements the aggregates of colloidal particles i.e. it produces the overgrowth that obscures original colloid particle shape. The vitreous silica that is common on the Orakei Korako terraces builds up in this way. While the deposit may appear hard and very adherent, it is microporous as not all the pores between the colloidal particles become infilled with silica. It is only with protracted, later-stage deposition of further silica that a deposit can be rendered relatively impervious.

6. ACKNOWLEDGMENTS

Thanks are due to Contact Energy for allowing access to and sampling of the Wairakei Power Station discharge drains and to Ruth Smith and Lew Bacon for supplying additional information and help. Phillipa and Craig Gibson kindly granted access to, and allowed sampling of, the sinter terraces at Orakei Korako. We *thank* Louise Cotterall for drafting the figures and Nisha Saheed for her help in preparing the manuscript.

7. REFERENCES

Herdianita, N.R., Browne, P.R.L., Rodgers, K.A. and Campbell, K.A. (2000a) Mineralogical and morphological changes accompanying aging of siliceous sinter and silica residue. *Mineralium Deposita 35(*1), 48-62.

Herdianita, N.R., Rodgers, K.A. and Browne, P.R.L. (2000b) Routine procedures for characterising modem and ancient silica sinter deposits. *Geothermics* 29(1), *65-8*1.

Iler, R.K. (1979) *The chemistry* of *silica: solubility, polymerization, colloid* and *surface properties, and biochemistry.* Wiley-Interscience, New York. 866p.

Landmesser, M. (1995) Mobilitiit durch Metastabilitiit: SiO_2 Transport und Akkumulation bei niedrigen Temperaturen. *Chemie der Erde* 55, 149-176.

Lloyd, E.F. (1972) Geology and hot springs of Orakeikorako. *New Zealand Geological Bulletin* 85, 1-164.

Rodgers, R.A. (2000) Research on silica sinters. *Mineralogical Society Bulletin* 126(April), 16-17.

Smith, D.K. (1998) Opal, cristobalite, and tridymite: noncrystallinity versus crystallinity, nomenclature of the silica minerals and bibliography. Powder *Diffraction*, 13(1), 2-19.

Table 1. Representative opal-A scattering band parameters

Group	Age - yrs	Location	Sample no'	Max intensity c/s	Max intensity Å	FWQM Å	FWHM Å	FWTM Å
A	≤0.1	Wairakei drain	Wkdrfresh6h	93	3.99	*0.80*	1.37	2.23
			Wkdrfresh3d	90	4.00	0.75	1.29	2.10
			Wkdrfresh5d	94	3.95	0.77	1.33	2.17
			Wkdrfresh16d	90	3.98	0.79	1.34	2.20
B	50.3	Ex Wairakei drain	Wkdrwal1	90	3.94	0.68	1.32	2.10
			Wkdrwal2	103	3.95	*0.84*	1.32	2.10
C	~0.1	Orakei Korako	S21(3)	102	4.00	0.80	1.40	2.16
	>1 and ≤2		Range of 6 samples	104-112	3.95-4.02	0.72-0.81	1.25-1.39	1.93-2.14

[1] h = hours; d = days